Available online at www.sciencedirect.com
ScienceDirect
Developmental Biology 308 (2007) 562–571
DEVELOPMENTAL BIOLOGY
www.elsevier.com/developmentalbiology

Genomes & Developmental Control

bHLH Transcription factors regulate organ morphogenesis via activation of an ADAMTS protease in *C. elegans*

Katsuyuki K. Tamai, Kiyoji Nishiwaki *

RIKEN Center for Developmental Biology, 2-2-3 Minatojima-minamimachi, Chuo-ku, Kobe 650-0047, Japan

Received for publication 1 March 2007; revised 26 April 2007; accepted 18 May 2007
Available online 25 May 2007

Abstract

The ADAMTS (a disintegrin and metalloprotease with thrombospondin motifs) family of secreted metalloproteases plays important roles in animal development and pathogenesis. However, transcriptional regulation of ADAMTS proteins during development remains largely unexplored. Here we show that basic helix–loop–helix (bHLH) transcription factors regulate the expression of an ADAMTS protease that is required for gonad development in *Caenorhabditis elegans*. Mutations in the gene *mig-24* cause shortened and swollen gonad arms due to a defect in gonadal leader cell migration, although leader cell specification appears to occur normally. The MIG-24 protein is a bHLH transcription factor of the Achaete–Scute family and is specifically expressed in gonadal leader cells. MIG-24 can physically interact with HLH-2, an E/Daughterless family bHLH transcription factor and bind the promoter region of *gon-1*, which encodes an ADAMTS protease required for gonadal leader cell migration. Mutations or RNA interference of *mig-24* and *hlh-2* severely impaired *gon-1* expression and forced expression of GON-1 in leader cells in *mig-24* mutants partially rescued the gonadal elongation defect. We propose that, unlike most previously characterized Achaete–Scute transcription factors that are involved in cell fate specification, MIG-24 acts with HLH-2 in specified cells to control cell migration by activating the expression of the GON-1 ADAMTS protease.

Keywords: ADAMTS protease; bHLH Transcription factor; GON-1; MIG-24; HLH-2; Organ morphogenesis; Cell migration

Introduction

The U-shape of the *Caenorhabditis elegans* gonad arms reflects the migration paths of the gonadal leader cells, distal tip cells (DTCs) in hermaphrodites and male linker cells (MLCs) in males, during larval development (Kimble and Hirsh, 1979). Studies on two secreted ADAMTS family metalloproteases, MIG-17 and GON-1, suggest that proteolytic remodeling of basement membranes of the gonad arms and/or the body wall is important for the correct migration of the gonadal leader cells. MIG-17 is secreted from the body wall muscle cells and localizes to the gonad surface where it controls the migratory direction of the gonadal leader cells (Nishiwaki et al., 2000), whereas GON-1 is secreted from both body wall muscle cells and gonadal leader cells and is required for morphogenesis of the gonad (Blelloch et al., 1999; Blelloch and Kimble, 1999). GON-1 secreted from DTCs is required for motility of the leader cells, whereas GON-1 secreted from body wall muscle cells is necessary for the expansion of the gonad along all axes.

Basic helix–loop–helix (bHLH) transcription factors have important roles in various biological phenomena such as myogenesis, neurogenesis, development of the heart and pancreas, and hypoxia response (Massari and Murre, 2000). Daughterless, an E protein ortholog in *Drosophila*, is required for sex determination, oogenesis, neurogenesis and differentiation of neural precursor cells (Brown et al., 1996; Hassan and Vaessin, 1997; Jafar-Nejad et al., 2006; Smith et al., 2001; Vaessin et al., 1994). The E/Daughterless proteins form dimers with other bHLH proteins through helix–loop–helix domains and bind to the E-box sequence, CANNTG, in the regulatory regions of target genes via basic domains (Bertrand et al., 2002). Furthermore, members of the Achaete–Scute family of bHLH proteins are key regulators of neural specification (Bertrand et

* Corresponding author. Fax: +81 78 306 3261.
E-mail address: nishiwak@cdb.riken.jp (K. Nishiwaki).

0012-1606/$ - see front matter © 2007 Elsevier Inc. All rights reserved.
doi:10.1016/j.ydbio.2007.05.024

al., 2002). Proteins of this family are characterized by tissue-specific expression profiles and formation of heterodimers with E/Daughterless proteins.

In *C. elegans*, HLH-2 is the sole ortholog of E/Daughterless proteins and functions with many other bHLH proteins. HLH-3, an Achaete–Scute family protein, forms a heterodimer with HLH-2 and activates *egl-1* to induce programmed cell death of the sister cells of pharyngeal neuro-secretory motor (NSM) neurons (Thellmann et al., 2003). HLH-2 also specifies mesodermal fate when complexed with HLH-8, a Twist ortholog (Harfe et al., 1998), promotes morphogenesis of sensory rays in males with LIN-32, a member of the Atonal family (Portman and Emmons, 2000), and specifies the PVQ/HSN/PHB neuroblast with HLH-14, a member of the Achaete–Scute family (Frank et al., 2003). Because HLH-2 is broadly expressed and is involved in many different cellular processes, the specificity of its transcriptional targets is often determined by its tissue-specific dimerization partners. Importantly, HLH-2 has been shown to be required for both DTC specification and function, as demonstrated by RNA interference (RNAi) analysis (Karp and Greenwald, 2004).

In the present study, we show that MIG-24, a novel bHLH transcription factor of the Achaete–Scute family, appears to act together with HLH-2 to regulate the migration of gonadal leader cells. MIG-24 is required for the expression of an ADAMTS metalloprotease, GON-1, which, in turn, is required for migration of gonadal leader cells (Blelloch et al., 1999). Unlike most previously characterized Achaete–Scute bHLH transcription factors, which have roles in cell fate specification, MIG-24 controls cell migration in specified cells.

Materials and methods

C. elegans genetics and molecular methods

Handling of worms was according to standard procedures (Brenner, 1974). The following mutations and genetic balancers were used: *unc-119(e2498)*, *unc-24(e138)*, *dpy-20(e1282)*, *hlh-2(bx108)*, *mig-24(k168, tk68)* (this work), *nT1[qIs51](IV; V)* and *hT2[qIs48](I; III)*. The *mig-24(k168)* mutant was generated by ethylmethane sulfonate mutagenesis. Three-factor mapping using *unc-24 dpy-20* and single nucleotide polymorphism mapping placed *mig-24* within 3.8 map units of linkage group IV. The cosmid clone C28C12 and a ~2.3-kb fragment containing a predicted gene *C28C12.8* rescued *mig-24(k168)* mutants. Based on the WormBase, *C28C12.8* is encoded within the sixth intron of a predicted gene *spp-10* that is orthologous to the human gene *PROSAPOSIN*. The *mig-24(tk68)* deletion mutant was isolated from a deletion mutant library constructed in our laboratory (Kubota et al., 2004). The *mig-24* and *hlh-2* cDNAs were synthesized using total RNA from wild-type worms with the 5′ RACE (rapid amplification of cDNA ends) System, Version 2.0 (GIBCO BRL Div. of Invitrogen, Gaithersburg, MD). L1-soaking RNAi was performed as described (Maeda et al., 2001). Microscopy was described by Kubota et al. (2004).

Plasmid construction

Promoter regions for *mig-24* (−1180 to +3), *lag-2* (−7388 to +3) and *unc-5* (−5129 to +3) were ligated to the *venus* or *mrfp* vector. The nucleotide positions are relative to the adenine residues of the initiation codons. The *venus* vector was a gift from Dr. Takeshi Ishihara at Kyushu University, Japan. The *mrfp* vector was provided by Roger Y. Tsien (Campbell et al., 2002). The coding region of the *gon-1* gene (+1 to +10709) was PCR amplified and ligated to the *lag-2* promoter. To assess the *gon-1* promoter activity, several truncated fragments (−12273 to +3, −8967 to +3, −4435 to +3, and −12273 to −7617) were fused to *venus*. The genomic coding regions of *mig-24* (+1 to +804) and *hlh-2* (+1 to +2665) were amplified and fused with the *hsp-16.2* promoter (−3034 to +3). Twelve E-boxes (CANNTG) at −11447, −11390, −11208, −11142, −10632, −10305, −10273, −10239, −10129, −10042, −9731, and −9216 in the *gon-1* promoter were mutated to AANNAG. Sequences of all PCR-amplified fragments were confirmed. Each plasmid construct was microinjected into host strains with marker plasmids *unc-119*$^{+}$ (20 to 50 ng/μl) and *sur-5*∷*gfp* (20 ng/μl in *lag-2p*∷*gon-1* transgenics) and pBluescript II KS(−) to bring total concentration to 200 ng/μl. Concentration (ng/μl) of test plasmids were *mig-24p*∷*venus* (150), *mig-24p*∷*mrfp* (50), *lag-2p*∷*venus* (10), *lag-2p*∷*mig-24*∷*venus* (5), *unc-5p*∷*venus* (50), *hsp-16.2p* plasmids (5), *gon-1p*∷*venus* constructs (25) and *lag-2p*∷*gon-1* (5).

Immunoprecipitation and immunoblotting

Mixed stage animals were heat shocked at 33 °C for 30 min. After recovery at 20 °C for 90 min, worms were collected and lysed in ice-cold lysis buffer (50 mM NaH_2PO_4, 50 mM NaCl, 1% (w/v) Triton X-100, protease inhibitor cocktail (Roche), and 1 mM phenylmethylsulfonyl fluoride) with glass beads. For immunoprecipitation, anti-c-Myc (goat IgG)-, anti-HA (goat IgG)-, and normal IgG (goat IgG)-conjugated agarose beads (BETHYL Laboratories, Inc.) were used. Immunoblotting was performed using anti-HA (rat monoclonal 3F10; Roche) and anti-c-Myc (mouse monoclonal 9E10; Sigma). HRP-linked anti-mouse IgG (Cell Signaling Technology, Inc.) and HRP-linked anti-rat IgG (Amersham Pharmacia Biotech) were used as secondary antibodies.

Chromatin immunoprecipitation (ChIP) analysis

The ChIP analysis (Nakayama et al., 2000) was modified for *C. elegans*. L2 and L3 stage worms were heat shocked as described above. Sonication was done until the chromatin was sheared into 200- to 500-bp fragments (Ultrasonic disruptor UD-201, TOMY) and immunoprecipitated. To detect the binding, multiplex PCR (37 cycles, 94 °C 30 s, 52 °C 20 s, 72 °C 30 s) was conducted using two primer sets: 5′-AAACGTTACAGTTACTGAGTGATTC-3′ and 5′-GCTCTCAAAAACCACCTAGTG-3′ for E-box, and 5′-TGATTTTTT-CACCGTAATGTTTC-3′ and 5′-ATCCAGATTGGTGAAAAACAG-3′ for GAPDH.

Results

MIG-24, an Achaete–Scute bHLH transcription factor, is required for gonadal leader cell migration

The *mig-24(k168)* mutant exhibited premature termination of DTC migration; 55% (n=60) of the anterior and 82% (n=60) of the posterior DTCs stopped prematurely (Figs. 1A, B, E). In many cases, the DTCs migrated diagonally rather than vertically along the lateral hypodermis and ceased to migrate over the dorsal muscle shortly after the second turn. The proximal gonadal arms were abnormally swollen with proliferating germ cells (Fig. 1B). Despite these severe gonad abnormalities, *mig-24(k168)* hermaphrodites could proliferate as homozygotes with small broods (Table S1). In males, the MLC leads the morphogenesis of the U-shaped gonad arm and disappears late in the L4 stage to connect the vas deferens to the proctodeum (Kimble and Hirsh, 1979). Fig. 1C shows a wild-type L4 male in which the MLC has almost reached the proctodeum. On the other hand, MLCs in the *mig-24* mutants prematurely ceased their migration and continued to exist even in adults, causing the gonad arms to be short and swollen (Fig.

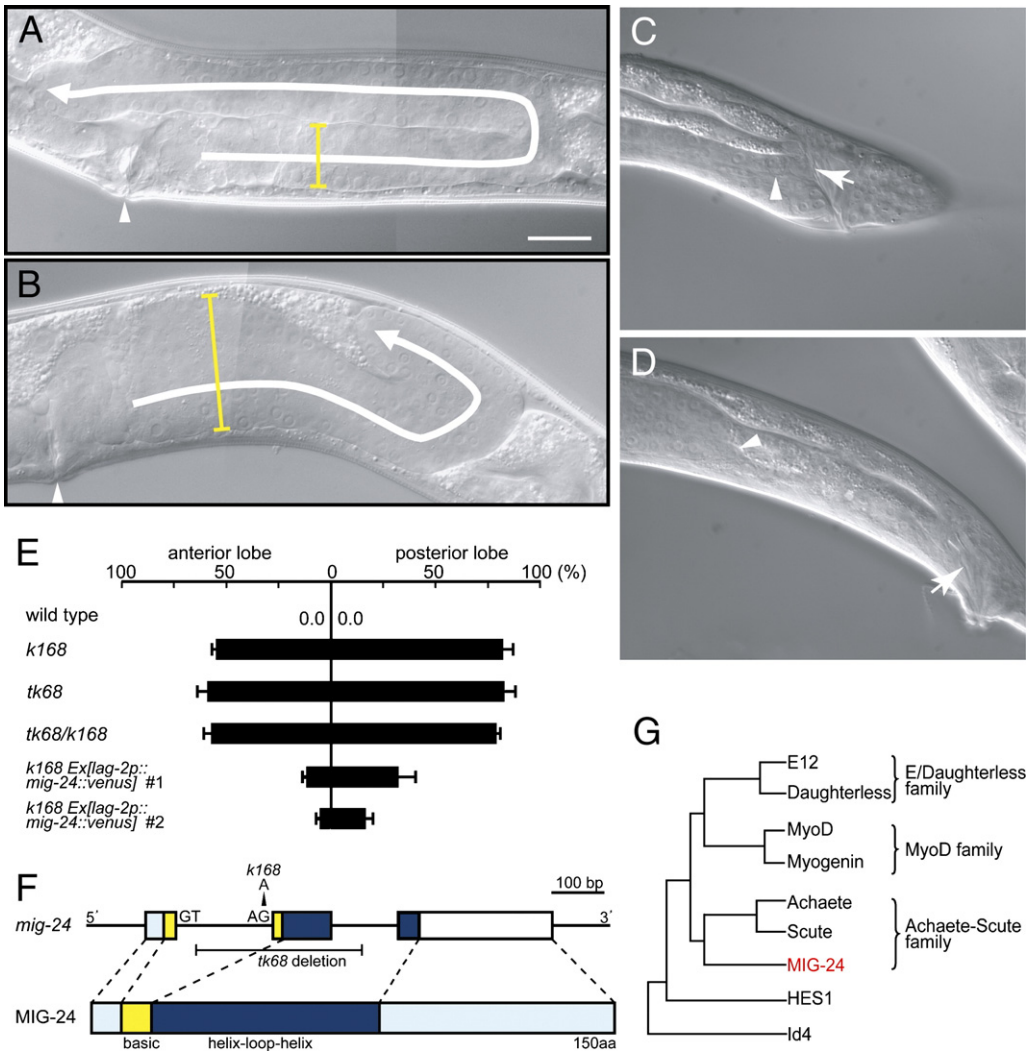

Fig. 1. Mutant phenotypes and gene structure of *mig-24*. (A, B) Nomarski images of the posterior gonads of wild-type (A) and *mig-24(k168)* (B) hermaphrodites. The migratory routes of DTCs are shown as white lines with arrowheads. Arrowheads indicate the position of the vulvae. In *mig-24* mutants, the DTCs often stop prematurely after the second turn, causing short and swollen gonadal arms. The width of the proximal gonad arms is shown by yellow bars. (C, D) MLCs (arrowheads) in a wild-type L4 male (C) and *mig-24(k168)* adult male (D). The MLC almost reaches the proctodeum (arrow) in the wild-type but is arrested far to the anterior in the *mig-24* mutant. Scale bar: 20 μm. (E) Percentage of wild-type animals, *mig-24(k168)* mutants, and two independent *mig-24(k168)* lines harboring *lag-2p::mig-24::Venus* extrachromosomal arrays with the premature termination phenotype for DTC migration. Premature termination represents arrest of DTC migration before reaching the vulva ($n=60$ for each experiment). Error bars represent SEM. (F) Structure of the *mig-24* gene and MIG-24 protein. The three exons of *mig-24* encode a bHLH transcription factor. The exon–intron composition was determined from genomic and cDNA sequences. The "G" in the acceptor sequence of the first intron was substituted with "A" in the *k168* mutation. The deleted region in *tk68* is shown. *mig-24* is equivalent to the predicted gene *hlh-12* (*C28C12.8*). (G) Comparison of bHLH domains of MIG-24 and other bHLH proteins. The phylogenetic tree was generated using the software Genetyx-Win 5.1.1 (Software Development Co., Ltd., Tokyo, Japan).

1D). This resulted in male sterility because of the absence of a passageway for sperm during ejaculation.

We cloned *mig-24* by positional mapping followed by transformation rescue. *mig-24* was predicted to comprise three exons encoding a member of the bHLH transcription factor family. RNAi of this transcription factor at the L1 stage phenocopied the DTC defect of *mig-24* mutants (Fig. S1). We discovered a mutation (from G to A) in the splice acceptor sequence of the first intron (Fig. 1F). Fig. 1G shows the phylogenetic tree of bHLH transcription factors for several organisms. Based on the amino acid sequence of the bHLH domain, MIG-24 is classified in the Achaete–Scute family (Fig. S2).

Expression of MIG-24 is restricted to gonadal leader cells

We examined the expression profile of *mig-24* by placing the Venus reporter gene (Nagai et al., 2002) under the control of the *mig-24* promoter (*mig-24p::venus*). The Venus expression began during the early L2 stage when DTCs start to migrate and was maintained specifically in DTCs until the adult stage (Figs. 2A, B). Although the signal was very faint, expression of the full-length *mig-24::venus* translational fusion construct in hermaphrodites, which fully rescues the *mig-24* phenotype, was detected only in DTC nuclei (data not shown). We also observed the expression pattern of *mig-24p::venus* in males, where the

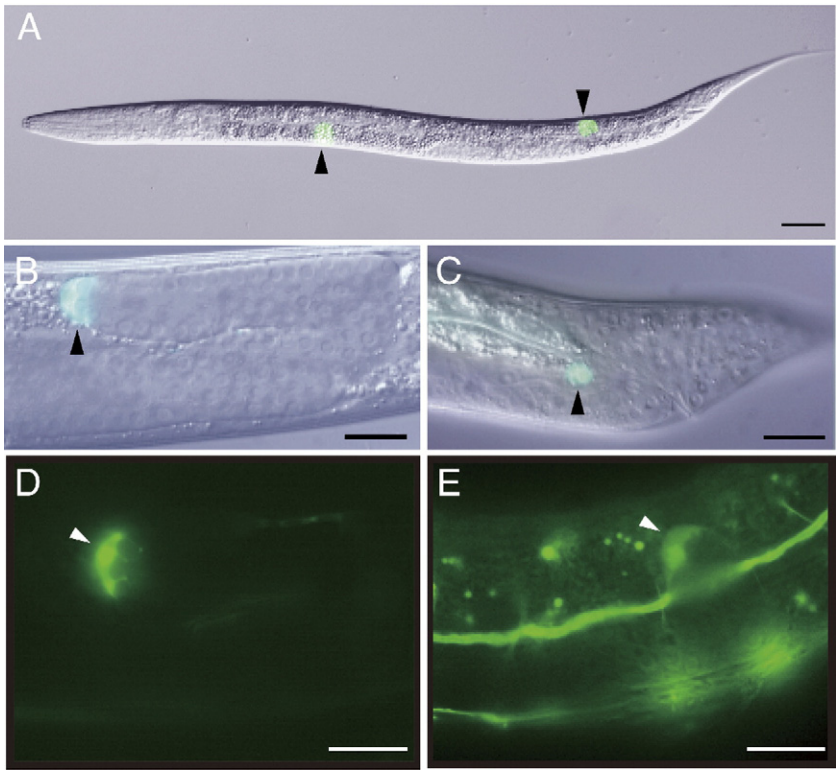

Fig. 2. MIG-24 is expressed specifically in gonadal leader cells. The pattern of MIG-24 expression was examined using the strain *unc-119 Ex[mig-24p*::*venus, unc-119*$^{+}$*]*. (A–C) The Venus signal was restricted to DTCs in hermaphrodites (A, L3; B, L4) and MLCs in males (C). Photos are merged images of Nomarski and fluorescence microscopy. (D, E) Expression of *lag-2p*::*venus* (D) and *unc-5p*::*venus* (E) in *mig-24(tk68)* hermaphrodites. Arrowheads indicate DTCs. Scale bars: 20 μm.

signal was detected specifically in MLCs from L2 through L4 stages (Fig. 2C). Thus, MIG-24 is expressed specifically in gonadal leader cells both in hermaphrodites and males. To examine whether MIG-24 functions cell autonomously in hermaphrodite DTCs, we expressed *mig-24*::*venus* from the *lag-2* gene promoter (*lag-2p*::*mig-24*::*venus*). The DTC migration defects were substantially suppressed in *mig-24(k168)* animals carrying *lag-2p*::*mig-24*::*venus* (Fig. 1E), suggesting that the function of MIG-24 is cell autonomous in the gonadal leader cells.

We generated a *mig-24* deletion mutant, *tk68*, in which most of the basic region and helix–loop–helix domain of MIG-24 are deleted (Fig. 1F) to create a putative null allele. This mutant was also homozygous fertile and gave a small brood size (Table S1). The phenotypic penetrance of premature termination of DTC migration in *tk68* homozygotes was comparable to those in *k168* homozygotes and *k168/tk68* heterozygotes (Fig. 1E). The premature termination phenotype could be attributed either to a normal migration rate of DTCs with earlier migration arrest or to a reduced DTC migration rate. To address this question, we examined the timing of turns of DTCs relative to the phases of vulval development. The vulval precursor cell P6.p undergoes three rounds of cell division and produces eight descendants that constitute the vulva. In the wild-type animal, most of the DTCs made the first turn over the ventral muscle at the four-P6.p cell stage, with 5% of DTCs making the first turn at the two-P6.p cell stage (Fig. 3). Although the first turn similarly occurred mostly at the four-P6.p cell stage in the mutants, 8% and 3% of DTCs turned at the eight-P6.p cell stage in *k168* and *tk68* mutants, respectively. In contrast to the wild-type DTCs, which always executed the second turn over the dorsal muscle

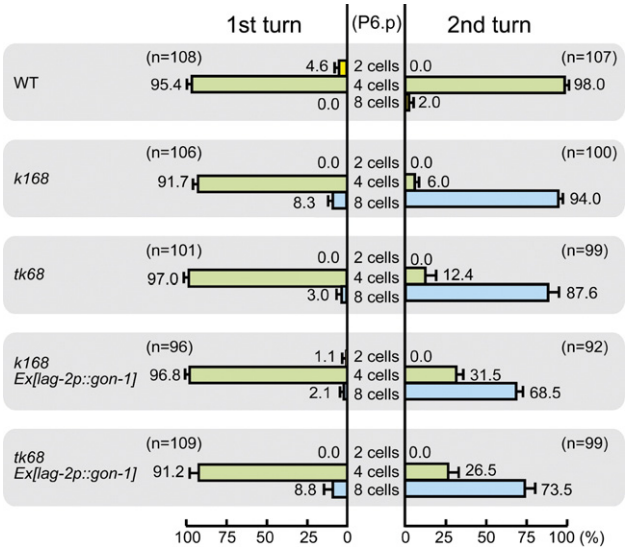

Fig. 3. Timing of reorientation of DTCs in wild-type and mutants. Animals with DTCs that were turning or just turned were selected and scored for their stages of vulval development (2, 4 or 8 P6.p cells). The left and right panels represent percentages of animals of the particular stages of vulval development at the first and the second turns, respectively. For the second turn, *p*-values for Fisher's Exact Test against the host strains were less than 0.01 for *k168 Ex[lag-2p*::*gon-1]* and less than 0.05 for *tk68 Ex[lag-2p*::*gon-1]*.

at the four-P6.p cell stage, DTCs in the *k168* and *tk68* mutants often made the second turn at the eight-P6.p cell stage. These results indicate that DTCs migrate slower in *mig-24* mutants than they do in the wild-type and suggest that MIG-24 has a minor role in promoting DTC migration before the first turn but an important role thereafter.

MIG-24 is not involved in gonadal leader cell specification

Because many bHLH proteins, including the Achaete–Scute family, function in cell fate determination, it is possible that MIG-24 is also involved in DTC specification. To assess this possibility, we first established the expression profile of *lag-2*, which encodes a GLP-1/Notch ligand and is expressed in differentiated DTCs to maintain the mitotic proliferation of germline stem cells (Henderson et al., 1994). We found that *lag-2p*::*venus* was strongly expressed in DTCs in *tk68* mutants from stage L1 through adulthood, as reported (Henderson et al., 1994) (Fig. 2D). We then assessed the expression of *unc-5* in DTCs, which encodes an UNC-6/netrin receptor required for the dorsal turn of DTCs in response to UNC-6 signal (Su et al., 2000). As shown in Fig. 2E, expression of the *unc-5p*::*venus* transgene began normally in DTCs of *tk68* animals when the DTCs began to reorient their migration toward the dorsal side (Su et al., 2000). Thus, DTCs in *mig-24* mutants are probably specified normally.

Genetic and physical interaction between MIG-24 and HLH-2

Members of the Achaete–Scute family of bHLH proteins form heterodimers with members of the E/Daughterless family of bHLH proteins in various organisms (Ferreiro et al., 1993; Murre et al., 1989; Thellmann et al., 2003). RNAi-mediated knockdown of *hlh-2*, the single *C. elegans* E/Daughterless ortholog, causes embryonic lethality or severe gonadal defects (Karp and Greenwald, 2004). We therefore investigated the interaction between MIG-24 and HLH-2. *hlh-2(bx108)*, a weak allele having a missense mutation in the HLH domain (Portman and Emmons, 2000), showed a subtle defect in DTC migration (Figs. 4A, C). When *hlh-2(bx108)* was combined with *mig-24 (k168)* or *mig-24(tk68)*, however, the double mutants exhibited very severe DTC migration defects (Figs. 4B, C). The DTCs often failed to make even the first turn (the no-turn phenotype) in the double mutants (Fig. 5), and the gonadal arms were short and swollen (Fig. 4B), resulting in sterility, despite the fact that a no-turn phenotype was observed in less than 8% of the anterior or posterior DTCs in *mig-24(k168)* or *mig-24(tk68)* single mutants. These synergistic effects are reminiscent of those observed for the ray morphogenesis phenotype when *lin-32* alleles were combined with *hlh-2(bx108)* (Portman and Emmons, 2000). *hlh-2(bx108)* has been suggested to be a hypomorphic allele that exhibits semidominance when combined with *lin-32* mutants—backgrounds in which ray morphogenesis is sensitized to the level of HLH-2 activity (Portman and Emmons, 2000). We examined whether *hlh-2 (bx108)* has a similar effect on DTC migration of *mig-24* mutants and found that *hlh-2(bx108)/+* also enhanced both the

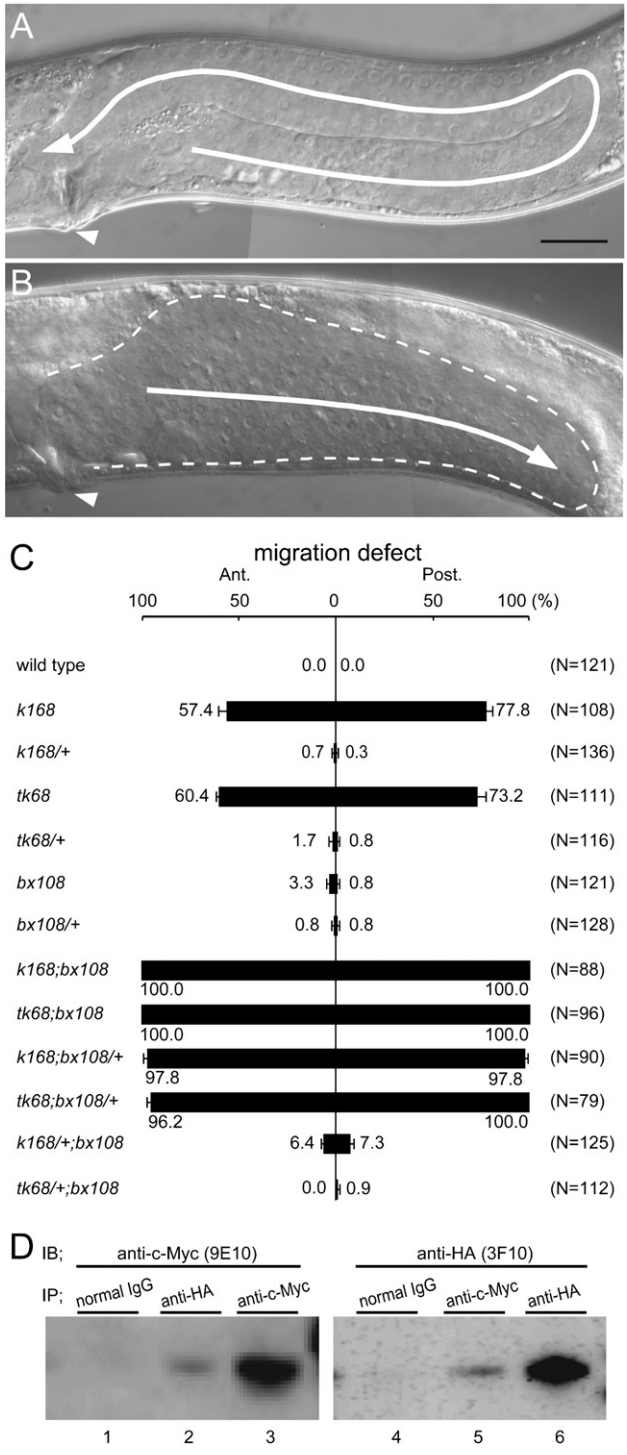

Fig. 4. Genetic interaction between *mig-24* and *hlh-2*. (A, B) Nomarski images of *hlh-2(bx108)* (A) and *mig-24(k168); hlh-2(bx108)* (B) adult hermaphrodites. Lines with arrowheads indicate the trajectory of DTC migration, and arrowheads indicate the position of the vulvae. Scale bar: 20 μm. (C) Percentages of animals with DTC migration defects in various mutant strains. Error bars represent SEM. (D) MIG-24 and HLH-2 physically interact. The strain *unc-119 Ex[hsp-16.2p*::*mig-24*::*3myc, hsp-16.2p*::*hlh-2*::*3ha, unc-119*$^{+}$*]* was heat shocked at 33 °C for 30 min, and the lysate was immunoprecipitated with anti-c-Myc or anti-HA-conjugated beads. MIG-24-3Myc was detected in lane 2, indicating that MIG-24-3Myc co-immunoprecipitated with HLH-2-3HA. Similarly, HLH-2-3HA was detected in lane 5, indicating that HLH-2-3HA co-immunoprecipitated with MIG-24-3Myc. Normal IgG was used as a control (lanes 1 and 4). These results were reproduced in two independent sets of experiments.

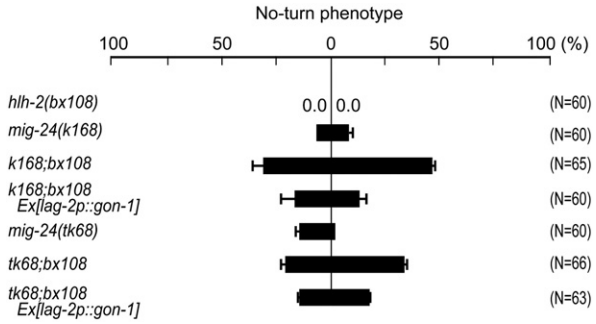

Fig. 5. Rescue of *mig-24; hlh-2* by *gon-1* expression in DTCs. Percentages of mutant and transgenic animals with the no-turn phenotype for DTC migration. *p*-Values for Fisher's Exact Test against the host strains were less than 0.001 for *k168; bx108 Ex[lag-2p::gon-1]* and less than 0.05 for *tk68; bx108 Ex[lag-2p::gon-1]*. Error bars represent SEM.

mig-24(k168) and *mig-24(tk68)* DTC migration defects (Fig. 4C). We then asked whether *mig-24* mutations conversely have a dominant effect in the *hlh-2(bx108)* background. Although both the *k168* and *tk68* mutation had very weak dominance over the *mig-24*$^{+}$ allele, only *k168* showed a further dominant effect on DTC migration in the *hlh-2(bx108)* background (Fig. 4C). These data indicate a complex genetic interaction between *mig-24* and *hlh-2* alleles, which will be discussed later.

We investigated whether MIG-24 and HLH-2 proteins physically interact. We placed *mig-24::3myc* and *hlh-2::3ha* fusion genes under the control of a heat-shocked promoter, *hsp-16.2p*, and these constructs were introduced into wild-type worms. After heat shock at 33 °C, a co-immunoprecipitation assay was performed. When MIG-24-3Myc was precipitated using anti-c-Myc, HLH-2-3HA was co-precipitated (Fig. 4D,

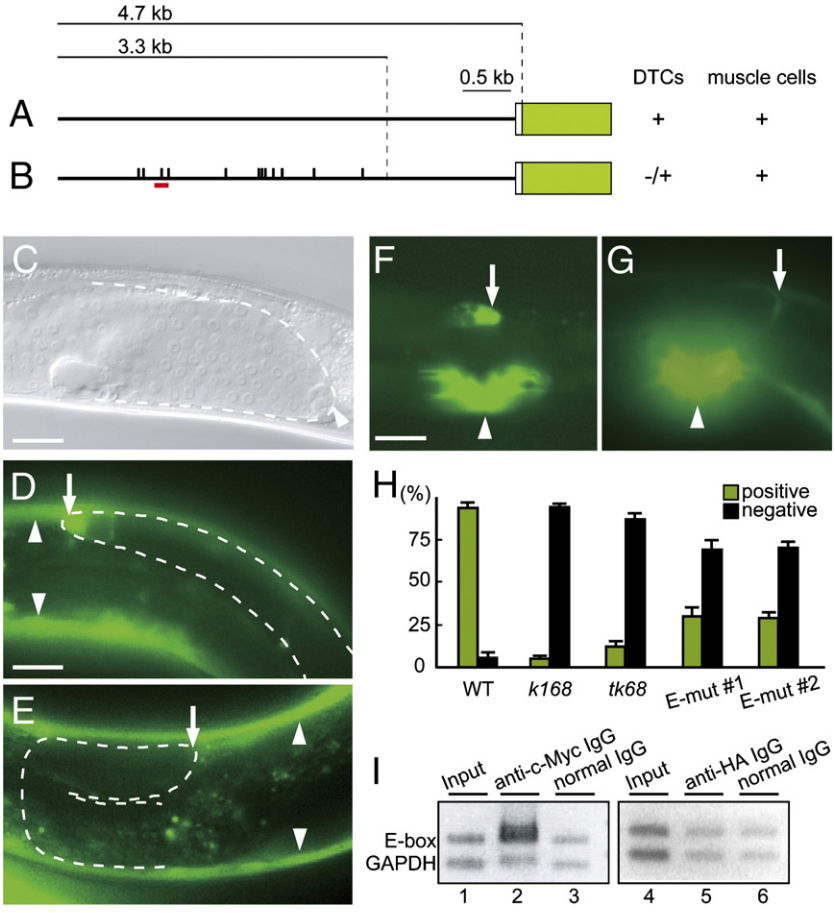

Fig. 6. *gon-1* expression in DTCs depends on MIG-24 activity. (A) An ~4.7-kb sequence, including exon 1 (white box), was fused to *venus* (green box). (B) Twelve potential E-boxes (vertical bars) in the 3.3-kb region were mutated. Venus expression in DTCs or muscle cells in wild-type transgenic animals is indicated by + or −. The red box represents the 238-bp region amplified in ChIP analysis (I). (C) A Nomarski image of the posterior gonad of *gon-1(e1254)*, a weak *gon-1* allele. Scale bar: 20 μm. (D, E) Expression of the construct shown in panel A. Venus expression was observed in both body wall muscles and DTCs in the wild type (D) but was remarkably reduced in DTCs only in *mig-24(k168)* (E). Scale bar: 20 μm. (F, G) Expression of constructs shown in panels A, F and panels B, G in wild-type animals. The disruption of the 12 potential E-boxes strongly reduced Venus expression in DTCs (arrows) without affecting its expression in vulval muscles (arrowheads). (H) Quantification of *gon-1* promoter activity in DTCs of wild-type and *mig-24* mutant animals having construct A and wild-type animals having construct B (E-mut #1 and E-mut #2, two independent lines). Green and black bars represent Venus expression scored as positive and negative, respectively. More than 50 DTCs were scored in each strain. Error bars represent SEM. (I) ChIP analysis. L2 and L3 larvae of strains *unc-119 Ex[hsp-16.2p::mig-24::3myc, hsp-16.2p::hlh-2::3ha, unc-119*$^{+}$*]* (left) and *unc-119; mig-24(tk68) Ex[hsp-16.2p::hlh-2::3ha, unc-119*$^{+}$*]* (right) were used. Input indicates the DNA samples before immunoprecipitation. Lysates were immunoprecipitated using anti-c-Myc (lane 2), anti-HA (lanes 5) or normal IgG (lanes 3 and 6). The precipitated DNA samples were amplified by multiplex PCR using both E-box- and GAPDH-specific primers. Heat shock expression of Myc and HA tagged proteins was confirmed by Western blots (data not shown). The results for ChIP analysis were reproduced in three independent sets of experiments.

lane 5). Likewise, MIG-24-3Myc was co-immunoprecipitated with HLH-2-3HA when anti-HA was used (Fig. 4D, lane 2). These results indicate that MIG-24 can form a heterodimer with HLH-2.

MIG-24 and HLH-2 activities and E-boxes are important for gon-1 expression

Because the short gonad arm phenotype of *mig-24; hlh-2* is reminiscent of that seen in the weak *gon-1* mutant *e1254* (Fig. 6C), we examined the possibility that *gon-1* is a transcriptional target of MIG-24. The secreted ADAMTS metalloprotease GON-1 is expressed in several tissues, including gonadal leader cells and body wall muscle cells (Blelloch and Kimble, 1999). Deletion analysis of the *gon-1* promoter region revealed that a 5′ 3.3-kb region of the 4.7-kb segment upstream from the transcriptional start site is sufficient for expression of a *gon-1p*::*venus* transcriptional fusion in both DTCs and muscles (Fig. 6A; Fig. S3). We used this promoter region to analyze *gon-1* expression.

In the wild-type background, Venus expression from the *gon-1* promoter was observed in DTCs, body wall muscles, vulval muscles and other tissues (Fig. 6D), as reported (Blelloch and Kimble, 1999). Although Venus expression was detected in 94% of DTCs in wild-type, it was very weakly detectable in about 5% and 12% of DTCs in *mig-24(k168)* and *mig-24(tk68)* animals, respectively (Fig. 6H), whereas expression in other tissues was unaffected (Fig. 6E). RNAi of *mig-24* also substantially weakened *gon-1p*::*venus* expression—Venus expression was observed in only 18% of DTCs ($n=71$) following *mig-24*-specific RNAi compared to 82% ($n=88$) in mock RNAi. In both mutant and RNAi analyses, Venus expression, when detected, was substantially lower than the control. These results indicate that *gon-1* expression in DTCs strongly depends on the activity of MIG-24. If *gon-1* is a target of MIG-24, we would expect that the expression of *gon-1* would commence after that of *mig-24*. Therefore, we examined the timing of *gon-1* expression relative to that of *mig-24* in DTCs using *mig-24p*::*mrfp* and *gon-1p*::*venus*. As expected, expression of Venus was always detected in DTCs that also expressed red fluorescent protein (mRFP) (Fig. 7). We then examined whether *hlh-2* is also required for *gon-1p*::*venus* expression. Because *hlh-2*-specific RNAi in embryos causes embryonic lethality (Karp and Greenwald, 2004), we performed soaking RNAi at stage L1. The percentage of DTCs with Venus expression was reduced to 27% ($n=100$) following *hlh-2*-specific RNAi compared to 97% of DTCs with Venus expression ($n=139$) in mock RNAi-treated animals. These results suggest that *hlh-2* is also involved in the expression of *gon-1*. *hlh-2*-specific RNAi resulted in 57% ($n=60$) no-turn phenotype, which is higher than the 30% ($n=120$) observed following *mig-24*-specific RNAi. This increased frequency of a no-turn phenotype might be due to partial failure of DTC specification in worms after *hlh-2*-specific RNAi (Karp and Greenwald, 2004).

In the 3.3-kb region, there are 12 potential E-box sequences (CANNTG), which are binding sites for bHLH transcription factors. We investigated whether these E-boxes are important

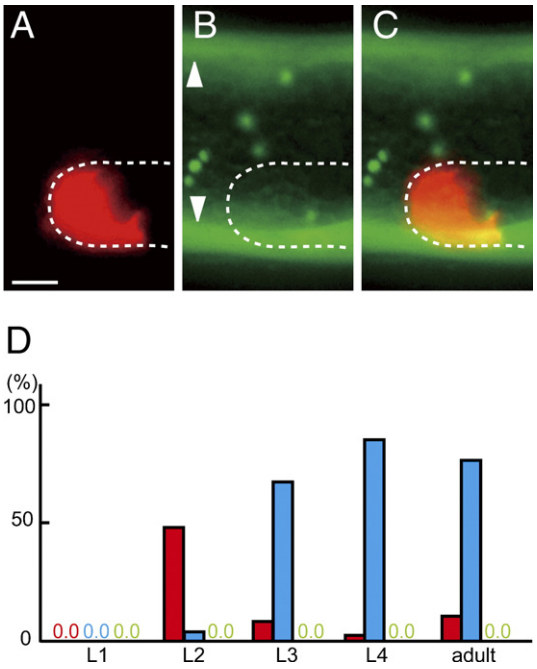

Fig. 7. Expression profiles of *mig-24* and *gon-1* during larval development. The strain *unc-119 Ex[mig-24p*::*mrfp, gon-1p*::*venus, unc-119*$^{+}$*]* was used. (A–C) Expression of *mig-24* and *gon-1* in an early L2 hermaphrodite. (A) mRFP was already expressed from *mig-24p*::*mrfp* (red). In the same animal, *gon-1p*::*venus* (green) is not expressed in the DTC but is expressed in body wall muscle cells arrowheads panel B. (C) A merged image. Dotted lines indicate the outline of the gonadal primordium. Scale bar: 5 μm. (D) Percentages of staged animals expressing mRFP only (red), both mRFP and Venus (blue), and Venus only (green). The animals positive for Venus expression were always positive for mRFP expression. Although it is possible that the time required for protein folding of mRFP and Venus is different, we observed that *mig-24* expression often turned on at the L2 stage, while *gon-1* kept mostly unexpressed at this stage using animals expressing either *mig-24p*::*venus* or *gon-1p*::*venus* (data not shown).

for *gon-1* expression in DTCs. All 12 E-boxes in the 3.3-kb region were mutated from CANNTG to AANNAG (Fig. 6B). These mutations substantially weakened *gon-1* promoter activity in DTCs, albeit without affecting the expression pattern in muscle cells (Figs. 6F, G); weak Venus expression was detectable in about 29% of DTCs in animals having the *gon-1* promoter with E-box mutations (Fig. 6H). These results indicate that the E-boxes are involved in transcriptional activation of *gon-1* in DTCs.

MIG-24 binds to the E-box sequence in the gon-1 promoter

To determine whether *gon-1* is the target of MIG-24, we investigated the ability of MIG-24 to bind to the *gon-1* promoter region. Of the 12 potential E-box sequences, the third, numbering from the 5′-end, has the sequence GCAGGTG, which is recognized by HLH-2/Daughterless of *C. elegans* and other organisms (Karp and Greenwald, 2003; Krause et al., 1997). To examine the binding of MIG-24 to this E-box in vivo, we performed a ChIP analysis using lysates of wild-type animals expressing both MIG-24-3Myc and HLH-2-3HA fusion proteins under a heat-shocked promoter. As shown in Fig. 6I, the

DNA fragment containing this E-box sequence of the *gon-1* promoter region co-immunoprecipitated much more efficiently with an antibody against Myc (lane 2) than with a control normal rabbit IgG (lane 3), suggesting that MIG-24-3Myc binds to the E-box-containing sequence in the *gon-1* promoter. As HLH-2 has been reported to bind the E-box sequence weakly as a homodimer (Portman and Emmons, 2000; Thellmann et al., 2003), we expressed HLH-2-3HA in the putative null *mig-24 (tk68)* background and examined its binding by ChIP analysis. However, we could not detect HLH-2 binding to the E-box-containing sequence (Fig. 6I, lane 5).

Artificial GON-1 expression in DTCs rescues DTC migration defects in mig-24 and mig-24; hlh-2 animals

If *gon-1* is the target of MIG-24, the artificial expression of GON-1 in DTCs should rescue the *gon-1*-like phenotype of *mig-24* and *mig-24; hlh-2* mutant animals. We placed the *gon-1* coding region under the *lag-2* promoter (*lag-2p*∷*gon-1*) and expressed this construct in these mutants. We examined the timing of DTC turns of *mig-24* mutants having *lag-2p*∷*gon-1*. The delay of the second turn in *k168* and *tk68* mutants was partially rescued by expressing GON-1 in DTCs, although rescue of the timing of the first turn was not obvious (Fig. 3). Also, the no-turn phenotype observed in *mig-24(k168); hlh-2 (bx108)* and *mig-24(tk68); hlh-2(bx108)* double mutants was partially ameliorated by GON-1 expression (Fig. 5). These results indicate that the elongation defect of gonadal arms in *mig-24* and *mig-24; hlh-2* mutants is partly caused by reduced expression of GON-1 in DTCs and strongly suggest that *gon-1* is a transcriptional target of MIG-24 and HLH-2.

Discussion

MIG-24 and other Achaete–Scute family proteins

Many Achaete–Scute members have a proneural function that is required for the generation of neuronal progenitors committed to differentiate and some Achaete–Scute proteins also act in differentiation of committed progenitors. For example, the *Drosophila* proneural gene *asense* is also required for the differentiation of sensory organs (Dominguez and Campuzano, 1993). Mash1 in mouse acts both in neurogenesis and migration of neural precursor cells (Ge et al., 2006). In *C. elegans*, HLH-3 and HLH-14 function both in commitment of neural precursor cells and their asymmetric cell divisions (Frank et al., 2003; Thellmann et al., 2003). Unlike most previously characterized Achaete–Scute members, however, MIG-24 appears to act purely to promote the migration of specified cells but not specification itself. This is supported by the fact that the expression of LAG-2 and UNC-5 is not affected in DTCs in *mig-24* mutants. In addition, expression of MIG-24 begins in DTCs several hours after their birth, and animals homozygous for the putative null *mig-24(tk68)* indeed proliferate, albeit very slowly. These observations further suggest that MIG-24 acts after the fate specification of DTCs. The expression of GON-1 could be considered to be one of the differentiated characteristics of DTCs and MIG-24 might be required to activate this particular process of differentiation.

Roles of MIG-24 and HLH-2 in DTC migration

MIG-24 is expressed specifically in DTCs when they initiate migration. The mechanism of initiating DTC migration is not known. As DTCs can start to migrate even in the *mig-24* mutant backgrounds, MIG-24 itself appears not to be involved in this mechanism. It may be possible that the mechanism to initiate DTC migration turns on the expression of MIG-24. In *Drosophila*, expression of *achaete–scute* complex is activated by a combination of transcription factors that prepattern the area of neural differentiation (Gomez-Skarmeta et al., 2003). Also, the expression of *achaete–scute* genes in particular neural precursors is maintained by autoregulation mediated by the binding of Achaete–Scute/Daughterless heterodimers to E-boxes within the promoters of *achaete–scute* genes (Culi and Modolell, 1998; Ramain et al., 2000). In the case of *mig-24*, however, because the *mig-24p*∷*venus* reporter is continuously expressed during DTC migration even in *mig-24* mutant backgrounds, such an autoregulatory mechanism does not appear to be in place.

We observed a complex genetic interaction between *mig-24* and *hlh-2* alleles. Because *tk68* is a putative null allele of *mig-24* and *hlh-2(bx108)* itself has a very weak DTC defect, the strong enhancement of DTC migration defects in *tk68; bx108* suggests that *hlh-2(bx108)* is defective in functions partially redundant with those of *mig-24* and therefore HLH-2 can function at least partly independent of MIG-24. The fact that the DTC phenotype of *tk68/+*, a heterozygote of a putative null allele, was not enhanced by *hlh-2(bx108)* suggests that a single *mig-24*$^{+}$ allele is sufficient to support normal DTC migration in the *hlh-2(bx108)* background. Thus, the allele-specific enhancement of DTC migration defects in *k168/+; bx108* suggests that *k168* is not a simple loss-of-function allele, but a gain-of-function allele that partially impairs the activity controlling DTC migration in the *hlh-2(bx108)* background. It might be possible that *mig-24(k168)* affects the ability of *mig-24*$^{+}$ or *hlh-2(bx108)* to control DTC migration. The stronger enhancing effect of *hlh-2(bx108)* on the no-turn phenotype of *k168* compared to that of *tk68* seems to reflect this gain-of-function nature of the *k168* allele. These genetic results are consistent with that HLH-2 might function with MIG-24 directly and have additional roles by itself or in combination with other bHLHs in DTC migration.

Roles of MIG-24 and HLH-2 in transcription of gon-1

We showed that the expression of *gon-1*, which encodes a secreted metalloprotease, is substantially decreased in *mig-24* mutants. Site-directed mutagenesis of E-boxes in the *gon-1* promoter region also substantially reduced *gon-1* expression, suggesting that MIG-24 acts in transcription of *gon-1* through the E-boxes. The biochemical evidence that MIG-24 binds the Daughterless homolog HLH-2 and an E-box-containing region of the *gon-1* promoter is consistent with the role of a MIG-24/HLH-2 heterodimer in *gon-1* transcription.

However, the fact that expression of *gon-1* was not completely abolished in DTCs of *mig-24(tk68)*, a putative null mutant, indicates weak *gon-1* transcriptional activity independent of MIG-24. Such weak activity might be attributable to other transcription factors including HLH-2 for the following reasons. First, the enhancement of the DTC migration defect of *mig-24(tk68)* by *hlh-2(bx108)* suggests that wild-type HLH-2 can control DTC migration in the absence of MIG-24. Second, *hlh-2*-specific RNAi markedly reduced *gon-1* expression in DTCs. Although we could not detect HLH-2 binding to an E-box region of *gon-1* with ChIP analysis, it has been reported that the HLH-2 homodimer weakly binds an E-box-containing sequence of *hlh-2* using electrophoretic mobility-shift assay (Portman and Emmons, 2000; Thellmann et al., 2003). Therefore, it might be possible that the in vivo binding of HLH-2 homodimers and the *gon-1* promoter is too weak to be detectable by ChIP analysis, but it is still sufficient to support the basal expression of *gon-1* in DTCs. It is not clear whether HLH-2 homodimers function in the wild-type *mig-24* background. Because DTC migration is nearly normal before their first turn in *mig-24(tk68)* animals, it is likely that basal expression of *gon-1* in the absence of MIG-24 is just sufficient to promote DTC migration during this phase.

We found that mutagenesis of all 12 E-boxes did not completely abolish *gon-1* expression in DTCs. A similar result was reported for the expression of *lag-2* in the anchor cell in animals with mutated *lag-2* E-boxes (Karp and Greenwald, 2003). The residual promoter activity may suggest that MIG-24/HLH-2 or HLH-2/HLH-2 also affects the transcription of *gon-1* through promoter regions other than the E-boxes. Alternatively, other transcription factors might be involved in the basal expression of *gon-1* in DTCs. Since GON-1 expression under the *lag-2* promoter only partially rescued the DTC migration defects in *mig-24* single and *mig-24; hlh-2* double mutants, MIG-24 and HLH-2 probably have targets other than *gon-1* that function during DTC migration.

We propose that MIG-24 and HLH-2 promote gonadal leader cell migration via transcriptional activation of *gon-1* and other target genes. MIG-24 is expressed specifically in leader cells at the L2 stage after their differentiation and may form a heterodimer with HLH-2, which is expressed in leader cells from late L1 (Karp and Greenwald, 2004) and bind to E-boxes to promote the transcription of *gon-1* and other target genes. HLH-2 homodimers may also act in this transcription. Secreted GON-1 degrades components of basement membranes on the gonad surface and/or the body wall to contribute to active migration of gonadal leader cells. It is possible that HLH-2 initially functions as a homodimer or in heterocomplexes with unknown proteins during the specification of leader cells and then acts in a heterodimer with MIG-24 to promote leader cell migration.

Transcriptional regulation of ADAMTS proteases

ADAMTS-9 and ADAMTS-20 are GON-1 orthologs in mammals (Somerville et al., 2003). ADAMTS-9 has activities that degrade proteoglycans such as aggrecan and versican and is expressed in various tissues (Somerville et al., 2003), but it remains to be clarified how *ADAMTS-9* expression is regulated during organ development. Transcriptional regulation of ADAMTS proteases probably modulates the structure of basement membranes or connective tissues during organogenesis and plays important roles in pathogenesis. We have presented a model with which we can further test the molecular mechanisms of regulated expression of ADAMTS proteases during organ formation.

Acknowledgments

We thank Alan Coulson for the cosmid clones, Jun-ichi Nakayama for the ChIP protocol, Rie Kuroki, Asami Sumitani, Nobuko Uodome for their technical assistance, and Kunihiro Matsumoto, Naoki Hisamoto, Yukihiko Kubota, Norio Suzuki, Shinji Ihara, and Kiyotaka Ohkura for critical reading of the manuscript. We also thank all members of the Laboratory for Cell Migration for their helpful discussions.

Appendix A. Supplementary data

Supplementary data associated with this article can be found, in the online version, at doi:10.1016/j.ydbio.2007.05.024.

References

Bertrand, N., Castro, D.S., Guillemot, F., 2002. Proneural genes and the specification of neural cell types. Nat. Rev., Neurosci. 3, 517–530.

Blelloch, R., Kimble, J., 1999. Control of organ shape by a secreted metalloprotease in the nematode *Caenorhabditis elegans*. Nature 399, 586–590.

Blelloch, R., Anna-Arriola, S.S., Gao, D., Li, Y., Hodgkin, J., Kimble, J., 1999. The *gon-1* gene is required for gonadal morphogenesis in *Caenorhabditis elegans*. Dev. Biol. 216, 382–393.

Brenner, S., 1974. The genetics of *Caenorhabditis elegans*. Genetics 77, 71–94.

Brown, N.L., Paddock, S.W., Sattler, C.A., Cronmiller, C., Thomas, B.J., Carroll, S.B., 1996. *daughterless* is required for *Drosophila* photoreceptor cell determination, eye morphogenesis, and cell cycle progression. Dev. Biol. 179, 65–78.

Campbell, R.E., Tour, O., Palmer, A.E., Steinbach, P.A., Baird, G.S., Zacharias, D.A., Tsien, R.Y., 2002. A monomeric red fluorescent protein. Proc. Natl. Acad. Sci. U. S. A. 99, 7877–7882.

Culi, J., Modolell, J., 1998. Proneural gene self-stimulation in neural precursors: an essential mechanism for sense organ development that is regulated by Notch signaling. Genes Dev. 12, 2036–2047.

Dominguez, M., Campuzano, S., 1993. *asense*, a member of the *Drosophila achaete–scute* complex, is a proneural differentiation gene. EMBO J. 12, 2049–2060.

Ferreiro, B., Skoglund, P., Bailey, A., Dorsky, R., Harris, W., 1993. *XASH1*, a *Xenopus* homolog of *achaete–scute*: a proneural gene in anterior regions of the vertebrate CNS. Mech. Dev. 40, 25–36.

Frank, C.A., Baum, P.D., Garriga, G., 2003. HLH-14 is a *C. elegans* Achaete–Scute protein that promotes neurogenesis through asymmetric cell division. Development 130, 6507–6518.

Ge, W., He, F., Kim, K.J., Blanchi, B., Coskun, V., Nguyen, L., Wu, X., Zhao, J., Heng, J.I.-T., Martinowich, K., Tao, J., Wu, H., Castro, D., Sobeih, M.M., Corfas, G., Gleeson, J.G., Greenberg, M.E., Guillemot, F., Sun, Y.E., 2006. Coupling of cell migration with neurogenesis by proneural bHLH factors. Proc. Natl. Acad. Sci. U. S. A. 103, 1319–1324.

Gomez-Skarmeta, J.L., Campuzano, S., Modolell, J., 2003. Half a century of neural prepatterning: the story of a few bristles and many genes. Nat. Rev., Neurosci. 4, 587–598.

Harfe, B.D., Gomes, A.V., Kenyon, C., Liu, J., Krause, M., Fire, A., 1998.

Analysis of a *Caenorhabditis elegans* Twist homolog identifies conserved and divergent aspects of mesodermal patterning. Genes Dev. 12, 2623–2635.

Hassan, B., Vaessin, H., 1997. Daughterless is required for the expression of cell cycle genes in peripheral nervous system precursors of *Drosophila* embryos. Dev. Genet. 21, 117–122.

Henderson, S., Gao, D., Lambie, E., Kimble, J., 1994. *lag-2* may encode a signaling ligand for the GLP-1 and LIN-12 receptors of *C. elegans*. Development 120, 2913–2924.

Jafar-Nejad, H., Tien, A.-C., Acar, M., Bellen, H.J., 2006. Senseless and Daughterless confer neuronal identity to epithelial cells in the *Drosophila* wing margin. Development 133, 1683–1692.

Karp, X., Greenwald, I., 2003. Post-transcriptional regulation of the E/Daughterless ortholog HLH-2, negative feedback, and birth order bias during the AC/VU decision in *C. elegans*. Genes Dev. 17, 3100–3111.

Karp, X., Greenwald, I., 2004. Multiple roles for the E/Daughterless ortholog HLH-2 during *C. elegans* gonadogenesis. Dev. Biol. 272, 460–469.

Kimble, J., Hirsh, D., 1979. The postembryonic cell lineages of the hermaphrodite and male gonads in *Caenorhabditis elegans*. Dev. Biol. 70, 396–417.

Krause, M., Park, M., Zhang, J., Yuan, J., Harfe, B., Xu, S., Greenwald, I., Cole, M., Paterson, B., Fire, A., 1997. A *C. elegans* E/Daughterless bHLH protein marks neuronal but not striated muscle development. Development 124, 2179–2189.

Kubota, Y., Kuroki, R., Nishiwaki, K., 2004. A fibulin-1 homolog interacts with an ADAM protease that controls cell migration in *C. elegans*. Curr. Biol. 14, 2011–2018.

Maeda, I., Kohara, Y., Yamamoto, M., Sugimoto, A., 2001. Large-scale analysis of gene function in *Caenorhabditis elegans* by high-throughput RNAi. Curr. Biol. 11, 171–176.

Massari, M.E., Murre, C., 2000. Helix–loop–helix proteins: regulators of transcription in eucaryotic organisms. Mol. Cell. Biol. 20, 429–440.

Murre, C., McCaw, P., Vaessin, H., Caudy, M., Jan, L., Cabrera, C., Buskin, J., Hauschka, S., Lassar, A., 1989. Interactions between heterologous helix–loop–helix proteins generate complexes that bind specifically to a common DNA sequence. Cell 58, 537–544.

Nagai, T., Ibata, K., Park, E.S., Kubota, M., Mikoshiba, K., Miyawaki, A., 2002. A variant of yellow fluorescent protein with fast and efficient maturation for cell-biological applications. Nat. Biotechnol. 20, 87–90.

Nakayama, J.-i., Klar, A.J.S., Grewal, S.I.S., 2000. A chromodomain protein, Swi6, performs imprinting functions in fission yeast during mitosis and meiosis. Cell 101, 307–317.

Nishiwaki, K., Hisamoto, N., Matsumoto, K., 2000. A metalloprotease disintegrin that controls cell migration in *Caenorhabditis elegans*. Science 288, 2205–2208.

Portman, D., Emmons, S., 2000. The basic helix–loop–helix transcription factors LIN-32 and HLH-2 function together in multiple steps of a *C. elegans* neuronal sublineage. Development 127, 5415–5426.

Ramain, P., Khechumian, R., Khechumian, K., Arbogast, N., Ackermann, C., Heitzler, P., 2000. Interactions between chip and the achaete/scute-daughterless heterodimers are required for pannier-driven proneural patterning. Mol. Cell 6, 781–790.

Smith III, J.E., Cronmiller, C., 2001. The *Drosophila daughterless* gene autoregulates and is controlled by both positive and negative *cis* regulation. Development 128, 4705–4714.

Somerville, R.P.T., Longpre, J.-M., Jungers, K.A., Engle, J.M., Ross, M., Evanko, S., Wight, T.N., Leduc, R., Apte, S.S., 2003. Characterization of ADAMTS-9 and ADAMTS-20 as a distinct ADAMTS subfamily related to *Caenorhabditis elegans* GON-1. J. Biol. Chem. 278, 9503–9513.

Su, M., Merz, D., Killeen, M., Zhou, Y., Zheng, H., Kramer, J., Hedgecock, E., Culotti, J., 2000. Regulation of the UNC-5 netrin receptor initiates the first reorientation of migrating distal tip cells in *Caenorhabditis elegans*. Development 127, 585–594.

Thellmann, M., Hatzold, J., Conradt, B., 2003. The Snail-like CES-1 protein of *C. elegans* can block the expression of the *BH3-only* cell-death activator gene *egl-1* by antagonizing the function of bHLH proteins. Development 130, 4057–4071.

Vaessin, H., Brand, M., Jan, L., Jan, Y., 1994. *daughterless* is essential for neuronal precursor differentiation but not for initiation of neuronal precursor formation in *Drosophila* embryo. Development 120, 935–945.